A Study on Fractional SIR Epidemic Model with Vital Dynamics and Variable Population Size using the Residual Power Series Method

Rakesh Kumar Meena[1], Sushil Kumar[2]
Department of Mathematics,
S. V. National Institute of Technology, Surat-395007 (Gujarat), India.
[1]rakeshkumarmeena318@gmail.com, [2]sushilk@amhd.svnit.ac.in

December 31, 2023

Abstract

In this paper, we develop an integer and fractional-order susceptible, infectious, and recovery (SIR) epidemic model based on vital dynamics, i.e., birth, death, immigration, and variable population size, including infection and recovery rates. We investigate the stability analysis for the fractional SIR model on the disease-free and endemic equilibrium points. The existence and uniqueness conditions of solutions for a stable model are also discussed. The residual power series (RPS) approach is used to get the semi-analytical solutions of the proposed model in the form of convergent fractional power series. The convergence analysis of the RPS method is also discussed. Numerical results demonstrate the effect of distinct fractional orders $\alpha \in (0, 1]$ on the population density. The obtained results are exciting and may be beneficial for medical experts to control the epidemic disease.
Keywords: SIR model, Caputo derivative, Fractional power series, and Residual power series.

1 Introduction

Fractional calculus is a powerful tool for the mathematical modelling of physical problems [1, 2, 3]. It has been applied in many research areas, such as science, economics, engineering, etc. Additionally, fractional differential equations in nonlinear dynamics have been studied by many researchers [4, 5, 6, 7]. In classical integer-order epidemic models, the disease spreads between compartments of the model with an equal chance. The rates of contact and illness transmission should be constant. A fractional derivative could replace a classical derivative to learn more about the dynamics of the model [8, 9, 10].

There is no long-lasting protection against several infectious illnesses. Some infections recover, and some people become susceptible after an infection. The SIR model studies this kind of illness. The schematic of the susceptible, infectious, and recovery (SIR) model is shown in Fig. 1. Here, $S(t)$, $I(t)$, and $R(t)$ represent the number of susceptible individuals, the number of infectious individuals, and the number of recovery individuals, respectively, at time t. λ is the number of births per unit time. μ_1, μ_2, and μ_3 are the numbers of immigration and deaths per unit of time for S, I, and R, respectively. r_1 and r_2 are the numbers of infectious people per infected person per unit of time and the number of recovered people per unit of time, respectively. The considered population size at time t is $N(t) = S(t) + I(t) + R(t)$.

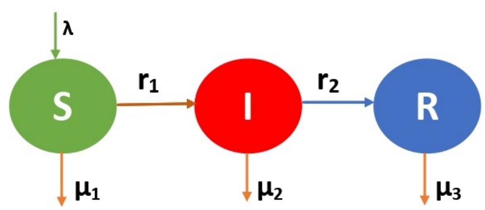

Figure 1: SIR Epidemic Model.

Researchers have successfully investigated several generalized variations of the classical and fractional-order epidemic models. Hethcote and Driessche [11] studied an susceptible-infectious-susceptible (SIS) epidemic model with variable population size. Ackleh and Allen [12] and Zaman et al. [13] discussed the SIR epidemic model with varying population sizes. El-Saka [14] addressed fractional epidemic models like SIR and susceptible-infectious-recovery-susceptible with varying population sizes. The SIR model with varying population sizes and continuous recruitment was examined by Bakare et al. [15]. Hassouna et al. [16] studied a fractional SIS epidemic model with varying population sizes. Fractional-order SIR epidemiological models were examined by Tafhvaei et al. [17]. Koziol et al. [18] discussed the influence of fractional order values on the dynamic properties of the SIR model. The SIR, susceptible-exposive-infectious-recovery, and susceptible-exposive-infective-asymptomatic-recovery models with fractional orders were reviewed by Chen et al. [19]. Balzotti et al. [20] studied the fractional SIS epidemic model with varying population sizes. Meena and Kumar [21, 22] discussed the fractional SIR and SIS epidemic models with constant population size. Sidi Ammi et al. [23] studied the diffusive SIR epidemic model described by reaction-diffusion equations involving a fractional derivative. A fractional SIR epidemic model with treatment cure rate was discussed by Sadki et al. [24].

The above-cited articles considered SIR models with constant population sizes. To the best of the author's knowledge, the study of the integer and fractional order SIR models, considering the model's vital dynamics and variable population size, is lacking in the literature. So, in this paper, we develop integer and fractional order SIR epidemic models consisting of susceptible, infectious, and recovery groups with birth, immigration, death, infection, and recovery rates for variable population sizes. Moreover, parameters (i.e., λ, μ_1, μ_2, and μ_3) are added to discuss more insight into the model's dynamics. These parameters are directly associated with particular groups and also affect the population sizes during the disease.

In the present study, we deal with the aforementioned integer and fractional-order SIR epidemic models. The linearization procedure is used to discuss the stability analysis of the fractional model with disease-free and endemic equilibrium points. The existence and uniqueness of the solutions for the stable model are also examined. Semi-analytical solutions of the proposed model are obtained in the form of a fast-convergent series with the help of the RPS method. The absolute errors between the semi-analytical and numerical solutions using the Runge-Kutta (RK) method for $\alpha = 1$ are obtained to show the RPS method's effectiveness. The effect of the fractional order (α) on population densities is also discussed. The numerical and graphical results show that this study can benefit researchers, policy-makers, and medical experts understand the dynamics of epidemic models.

The structure of the paper is as follows: After the introduction in Section 1, some basic definitions of fractional calculus are listed in Section 2. A mathematical model is formulated in Section 3. The stability and existence of a uniformly stable solution for the proposed model are discussed in Section 4 and Section 5, respectively. Section 6 discusses the procedures of the RPS Method and the solution of the model. Numerical results and graphs are discussed in Section 7, and the outcomes of the study are concluded in Section 8.

2 Preliminaries

This section discusses the definitions and properties of fractional calculus. The fractional derivative has a variety of fascinating definitions. Yet, given their advantage over issues with an initial value, we use the well-known Caputo derivatives in the present study.

Definition 2.1 *[25] The Caputo fractional derivative of order α of function $r(y)$ is defined as:*

$$
{}_0^C D_y^\alpha r(y) = \begin{cases} \dfrac{1}{\Gamma(q-\alpha)} \displaystyle\int_0^y \frac{r^{(q)}(v)}{(y-v)^{\alpha+1-q}} dv, & \text{if } (q-1) < \alpha < q, \ q \in \mathbb{N}, \\ \dfrac{d^q}{dy^q} r(y), & \text{if } \alpha = q, \ q \in \mathbb{N}. \end{cases}
$$

Definition 2.2 *[26, 27] The fractional power series (FPS) about $y = y_0$ can be*

3

defined as

$$\sum_{j=0}^{\infty} l_j (y-y_0)^{j\alpha} = l_0 + l_1(y-y_0)^{\alpha} + l_2(y-y_0)^{2\alpha} + \dots;$$

$(q-1) < \alpha \leq q,\ q \in N,\ y \geq y_0$. *Where* $l_j,\ j = 0,1,2,\dots$ *are the coefficients of the FPS.*

Theorem 2.1 *[26, 27] A FPS of the function $r(y)$ about $y = y_0$ can be defined as*

$$r(y) = \sum_{j=0}^{\infty} l_j (y-y_0)^{j\alpha},\ y_0 \leq y < (y_0+\rho).$$

It was found that if ${}_0^C D_{y_0}^{j\alpha} r(y),\ \forall j = 0,1,2,\dots$ *are continuous on* $(y_0, y_0+\rho)$, *then* $l_j = \dfrac{D_{y_0}^{j} r(y_0)}{\Gamma(1+j\alpha)}$. *Where ρ is the radius of convergence and* ${}_0^C D_{y_0}^{j\alpha} = {}_0^C D_{y_0}^{\alpha}\, {}_0^C D_{y_0}^{\alpha} \dots {}_0^C D_{y_0}^{\alpha}$ *(j-times).*

Property 2.1 *[25] Let $r(y) = y^q$, $q \geq 0$,*

$${}_0^C D_y^{\alpha} y^q = \begin{cases} \dfrac{\Gamma(q+1)}{\Gamma(q+1-\alpha)} y^{q-\alpha}, & \text{if } q \geq \lceil \alpha \rceil, \\ 0, & \text{if } q < \lceil \alpha \rceil. \end{cases}$$

3 Mathematical Model

A mathematical model is vital in analyzing the physical, chemical, linguistic, etc., systems. The SIR model is general and can be used for the mathematical study of any disease like influenza, measles, chicken pox, mumps, etc. The assumption of a fractional-order SIR model in the epidemic has essential implications for the time domain. The fractional order model gives a better way to understand the physical behavior of the SIR epidemic model than the integer order model. Following are the assumptions to construct the SIR epidemic model at time t.

3.1 Assumptions

1. The disease spreads in a particular region with a variable population size $N(t)$, i.e., $S(t) + I(t) + R(t) = N(t)$.

2. $r_1 S(t) I(t)$ is total newly infected people from susceptible at time t.

3. $r_2 I(t)$ is the number of recovered infected persons at time t. The recovered person has ongoing immunity.

4. The number of births per unit of time t in the susceptible compartment is $\lambda N(t)$ at the rate λ.

5. The number of deaths and immigration in susceptible, infectious, and recovered compartments is $\mu_1 S(t)$, $\mu_2 I(t)$, and $\mu_3 R(t)$, respectively, with rates of μ_1, μ_2, and μ_3.

For integer order, the SIR model with vital dynamics can be formulated as

$$\left.\begin{aligned}
\frac{dS(t)}{dt} &= \lambda N(t) - r_1 S(t)I(t) - \mu_1 S(t),\\
\frac{dI(t)}{dt} &= r_1 S(t)I(t) - r_2 I(t) - \mu_2 I(t),\\
\frac{dR(t)}{dt} &= r_2 I(t) - \mu_3 R(t),\\
\frac{dS(t)}{dt} + \frac{dI(t)}{dt} + \frac{dR(t)}{dt} &= \frac{dN(t)}{dt}.
\end{aligned}\right\} \tag{1}$$

At $t = 0$, the initial conditions of the model (Eq. (1)) are given as

$$S(0) = S_0,\ I(0) = I_0,\ R(0) = R_0,\ \text{and}\ N(0) = N_0. \tag{2}$$

By replacing the integer order derivative with the Caputo derivatives of order $\alpha \in (0,1]$ in model (Eq. (1)), we have the following model

$$\left.\begin{aligned}
&{}_0^C D_t^\alpha S(t) = \lambda N(t) - r_1 S(t)I(t) - \mu_1 S(t),\\
&{}_0^C D_t^\alpha I(t) = r_1 S(t)I(t) - r_2 I(t) - \mu_2 I(t),\\
&{}_0^C D_t^\alpha R(t) = r_2 I(t) - \mu_3 R(t),\\
&{}_0^C D_t^\alpha S(t) + {}_0^C D_t^\alpha I(t) + {}_0^C D_t^\alpha R(t) = {}_0^C D_t^\alpha N(t).
\end{aligned}\right\} \tag{3}$$

At $t = 0$, the initial conditions of the model (Eq. (3)) are

$$S(0) = S_0,\ I(0) = I_0,\ R(0) = R_0,\ \text{and}\ N(0) = N_0. \tag{4}$$

Where parameters r_1, r_2, λ, μ_1, μ_2, and μ_3 are the positive constants.

4 Stability Analysis of the Fractional SIR Epidemic Model

In this section, we discuss disease-free and endemic equilibrium points of the model (Eq. (3)) as

$${}_0^C D_t^\alpha S(t) = 0,\ {}_0^C D_t^\alpha I(t) = 0,\ {}_0^C D_t^\alpha R(t) = 0.$$

4.1 Disease-free Equilibrium Point

The disease-free equilibrium point (i.e., $I = 0$) is $(S_{Eq}, I_{Eq}, R_{Eq}) = (0, 0, 0)$. We find matrix

$$A = \begin{bmatrix} \lambda - \mu_1 & \lambda & \lambda \\ 0 & -(r_2 + \mu_2) & 0 \\ 0 & r_2 & -\mu_3 \end{bmatrix}$$

and its eigenvalues are

$$\lambda_1 = \lambda - \mu_1,$$
$$\lambda_2 = -r_2 - \mu_2,$$
$$\lambda_3 = -\mu_3.$$

Hence, (S_{Eq}, I_{Eq}, R_{Eq}) is local asymptotically stable if $(\lambda - \mu_1) < 0$.

4.2 Endemic Equilibrium Point

The endemic equilibrium point $(S_{Eq}, I_{Eq}, R_{Eq}) = (S_\star, I_\star, R_\star)$, which is characterized by the existence of infected nodes, i.e., $I \neq 0$ is given as

$$S_\star = \frac{r_2 + \mu_2}{r_1}, I_\star = \frac{\mu_3(\mu_1 - \lambda)(r_2 + \mu_2)}{r_1\left[(\lambda - r_2 - \mu_2) * \mu_3 - \lambda r_2\right]}, R_\star = \frac{r_2(\mu_1 - \lambda)(r_2 + \mu_2)}{r_1\left[(\lambda - r_2 - \mu_2) * \mu_3 - \lambda r_2\right]}.$$

We find matrix

$$A = \begin{bmatrix} \lambda - \mu_1 - \dfrac{\mu_3(r_2 + \mu_2)(\lambda - \mu_1)}{r_2 + \mu_3(r_2 + \mu_1 - \lambda)} & \lambda - r_2 - \mu_2 & \lambda \\ \dfrac{\mu_3(r_2 + \mu_2)(\lambda - \mu_1)}{r_2 + \mu_3(r_2 + \mu_1 - \lambda)} & 0 & 0 \\ 0 & r_2 & -\mu_3 \end{bmatrix}$$

and if real parts of its all eigenvalues of matrix A are negative, then (S_{Eq}, I_{Eq}, R_{Eq}) is local asymptotically stable.

5 Existence and Uniqueness of Stable Solution

Let $y_1(t) = S(t)$, $y_2(t) = I(t)$, and $y_3(t) = R(t)$, then

$$f_1(y_1(t), y_2(t), y_3(t)) = (\lambda - \mu_1)y_1(t) - (\lambda + r_1 y_1(t))y_2(t) - \lambda y_3(t),$$
$$f_2(y_1(t), y_2(t), y_3(t)) = r_1 y_1(t) y_2(t) - (r_2 + \mu_2)y_2(t),$$
$$f_3(y_1(t), y_2(t), y_3(t)) = r_2 y_2(t) - \mu_3 y_3(t).$$

Let $D = \{y_1, y_2, y_3 \in R : |y_i(t)| \leq a, t \in [0, \rho]\}$ and $|f_i(y_1(t), y_2(t), y_3(t))| \leq M_i$, $i = 1, 2, 3$. Each function f_1, f_2, and f_3 is continuous with respect to the three parameters y_1, y_2, and y_3. Then on D we have

$$\left|\frac{\partial}{\partial y_1} f_1(y_1, y_2, y_3)\right| \leq k_1, \quad \left|\frac{\partial}{\partial y_2} f_1(y_1, y_2, y_3)\right| \leq k_2, \quad \left|\frac{\partial}{\partial y_3} f_1(y_1, y_2, y_3)\right| \leq k_3,$$
$$\left|\frac{\partial}{\partial y_1} f_2(y_1, y_2, y_3)\right| \leq l_1, \quad \left|\frac{\partial}{\partial y_2} f_2(y_1, y_2, y_3)\right| \leq l_2, \quad \left|\frac{\partial}{\partial y_3} f_2(y_1, y_2, y_3)\right| \leq l_3,$$
$$\left|\frac{\partial}{\partial y_1} f_3(y_1, y_2, y_3)\right| \leq m_1, \quad \left|\frac{\partial}{\partial y_2} f_3(y_1, y_2, y_3)\right| \leq m_2, \quad \left|\frac{\partial}{\partial y_3} f_3(y_1, y_2, y_3)\right| \leq m_3,$$

where k_i, l_i, and m_i, $i = 1, 2, 3$ are positive constants.
Consider the following initial value problem which represents the proposed model (Eq. (3))

$$\begin{aligned} {}_0^C D_t^\alpha y_1(t) &= f_1(y_1(t), y_2(t), y_3(t)),\ t > 0,\ \text{and}\ y_1(0) = y_{10}, \\ {}_0^C D_t^\alpha y_2(t) &= f_2(y_1(t), y_2(t), y_3(t)),\ t > 0,\ \text{and}\ y_2(0) = y_{20}, \\ {}_0^C D_t^\alpha y_3(t) &= f_3(y_1(t), y_2(t), y_3(t)),\ t > 0,\ \text{and}\ y_3(0) = y_{30}. \end{aligned} \tag{5}$$

Definition 5.1 *By a solution of the system (Eq. (5)), we mean a column vector* $(y_1(t), y_2(t), y_3(t))^\tau$, y_1, y_2, *and* $y_3 \in C[0,T]$, $T < \infty$ *where* $C[0,T]$ *is the class of continuous functions defined on the interval* $[0,T]$ *and* τ *denote the transpose of the matrix, and*

$$F(Y(t)) = (f_1(y_1(t), y_2(t), y_3(t)), f_2(y_1(t), y_2(t), y_3(t)), f_3(y_1(t), y_2(t), y_3(t)))^\tau.$$

Now, applying Theorem 2.1 [28], we deduce that the considered system has a unique solution. Also, this solution is uniformly Lyapunov stable by Theorem 3.2 [28].

6 Solution using RPS Method

6.1 RPS Methodology

In this section, we apply the RPS method [21, 29, 30, 31, 32, 33] to solve the proposed model (Eq. (3)) using following steps

Step 1: The FPS for $S(t)$, $I(t)$, $R(t)$, and $N(t)$ about $t = 0$ can be written as

$$\left.\begin{aligned} S(t) &= \sum_{j=0}^{\infty} \frac{a_j t^{j\alpha}}{\Gamma(j\alpha+1)}, \quad I(t) = \sum_{j=0}^{\infty} \frac{b_j t^{j\alpha}}{\Gamma(j\alpha+1)}, \\ R(t) &= \sum_{j=0}^{\infty} \frac{c_j t^{j\alpha}}{\Gamma(j\alpha+1)}, \quad N(t) = \sum_{j=0}^{\infty} \frac{d_j t^{j\alpha}}{\Gamma(j\alpha+1)}, \end{aligned}\right\} 0 \le t < \rho. \tag{6}$$

The n^{th}-truncated series of $S(t)$, $I(t)$, $R(t)$, and $N(t)$ denoted by $S_n(t)$, $I_n(t)$, $R_n(t)$, and $N_n(t)$, respectively, are defined as

$$\left.\begin{aligned} S_n(t) &= \sum_{j=0}^{n} \frac{a_j t^{j\alpha}}{\Gamma(j\alpha+1)}, \quad I_n(t) = \sum_{j=0}^{n} \frac{b_j t^{j\alpha}}{\Gamma(j\alpha+1)}, \\ R_n(t) &= \sum_{j=0}^{n} \frac{c_j t^{j\alpha}}{\Gamma(j\alpha+1)}, \quad N_n(t) = \sum_{j=0}^{n} \frac{d_j t^{j\alpha}}{\Gamma(j\alpha+1)}, \end{aligned}\right\} 0 \le t < \rho. \tag{7}$$

For $n = 0$, from Eqs. (4) and (7), we obtain

$$\begin{aligned} S_0(t) &= a_0 = S_0(0) = S_0, \quad I_0(t) = b_0 = I_0(0) = I_0, \\ R_0(t) &= c_0 = R_0(0) = R_0, \quad N_0(t) = d_0 = N_0(0) = N_0. \end{aligned} \tag{8}$$

7

Now, from Eqs. (7) and (8) the n^{th}-truncated series of Eq. (7) can be defined as

$$
\begin{aligned}
S_n(t) &= a_0 + \sum_{j=1}^{n} \frac{a_j t^{j\alpha}}{\Gamma(j\alpha+1)}, \quad I_n(t) = b_0 + \sum_{j=1}^{n} \frac{b_j t^{j\alpha}}{\Gamma(j\alpha+1)}, \\
R_n(t) &= c_0 + \sum_{j=1}^{n} \frac{c_j t^{j\alpha}}{\Gamma(j\alpha+1)}, \quad N_n(t) = d_0 + \sum_{j=1}^{n} \frac{d_j t^{j\alpha}}{\Gamma(j\alpha+1)}.
\end{aligned} \tag{9}
$$

Step 2: Define the residual functions for model (Eq. (3)) as

$$
\left.
\begin{aligned}
Res_S(t) &= {}_0^{\mathbf{C}}D_t^{\alpha} S(t) - \lambda N(t) + r_1 S(t) I(t) + \mu_1 S(t), \\
Res_I(t) &= {}_0^{\mathbf{C}}D_t^{\alpha} I(t) - r_1 S(t) I(t) + (r_2 + \mu_2) I(t), \\
Res_R(t) &= {}_0^{\mathbf{C}}D_t^{\alpha} R(t) - r_2 I(t) + \mu_3 R(t), \\
Res_N(t) &= {}_0^{\mathbf{C}}D_t^{\alpha} N(t) - \lambda N(t) + \mu_1 S(t) + \mu_2 I(t) + \mu_3 R(t).
\end{aligned}
\right\} \tag{10}
$$

Hence, the n^{th}-residual functions of $S(t)$, $I(t)$, $R(t)$, and $N(t)$, respectively, are

$$
\left.
\begin{aligned}
Res_{S_n}(t) &= {}_0^{\mathbf{C}}D_t^{\alpha} S_n(t) - \lambda N_n(t) + r_1 S_n(t) I_n(t) + \mu_1 S_n(t), \\
Res_{I_n}(t) &= {}_0^{\mathbf{C}}D_t^{\alpha} I_n(t) - r_1 S_n(t) I_n(t) + (r_2 + \mu_2) I_n(t), \\
Res_{R_n}(t) &= {}_0^{\mathbf{C}}D_t^{\alpha} R_n(t) - r_2 I_n(t) + \mu_3 R_n(t), \\
Res_{N_n}(t) &= {}_0^{\mathbf{C}}D_t^{\alpha} N_n(t) - \lambda N_n(t) + \mu_1 S_n(t) + \mu_2 I_n(t) + \mu_3 R_n(t).
\end{aligned}
\right\} \tag{11}
$$

The residual function satisfies the properties, $Res_S(t) = Res_I(t) = Res_R(t) = Res_N(t) = 0,\ \forall t \geq 0$. Also,

$$
\begin{aligned}
\lim_{n\to\infty} Res_{S_n}(t) &= Res_S(t), \quad \lim_{n\to\infty} Res_{I_n}(t) = Res_I(t), \\
\lim_{n\to\infty} Res_{R_n}(t) &= Res_R(t), \quad \lim_{n\to\infty} Res_{N_n}(t) = Res_N(t).
\end{aligned}
$$

From [29], we have

$$
\left.
\begin{aligned}
{}_0^{\mathbf{C}}D_t^{(j-1)\alpha} Res_S(0) &= {}_0^{\mathbf{C}}D_t^{(j-1)\alpha} Res_{S_i}(0), \\
{}_0^{\mathbf{C}}D_t^{(j-1)\alpha} Res_I(0) &= {}_0^{\mathbf{C}}D_t^{(j-1)\alpha} Res_{I_i}(0), \\
{}_0^{\mathbf{C}}D_t^{(j-1)\alpha} Res_R(0) &= {}_0^{\mathbf{C}}D_t^{(j-1)\alpha} Res_{R_i}(0), \\
{}_0^{\mathbf{C}}D_t^{(j-1)\alpha} Res_N(0) &= {}_0^{\mathbf{C}}D_t^{(j-1)\alpha} Res_{N_i}(0),
\end{aligned}
\right\} \forall j = 1, \ldots, n.
$$

Step 3: To determine the coefficients a_j, b_j, c_j, and d_j for $j = 1, 2, 3, \ldots, n$, we substitute the n^{th}-truncated series of $S(t)$, $I(t)$, $R(t)$, and $N(t)$ in Eq. (11), and then use the Caputo fractional derivative operator $D_0^{(n-1)\alpha}$

on $Res_S(t)$, $Res_I(t)$, $Res_R(t)$, and $Res_N(t)$. It gives the equations

$$\left.\begin{aligned} {}_0^{\mathbf{C}}D_t^{(n-1)\alpha} Res_S(0) = {}_0^{\mathbf{C}}D_t^{(n-1)\alpha} Res_{S_n}(0) = 0, \\ {}_0^{\mathbf{C}}D_t^{(n-1)\alpha} Res_I(0) = {}_0^{\mathbf{C}}D_t^{(n-1)\alpha} Res_{I_n}(0) = 0, \\ {}_0^{\mathbf{C}}D_t^{(n-1)\alpha} Res_R(0) = {}_0^{\mathbf{C}}D_t^{(n-1)\alpha} Res_{R_n}(0) = 0, \\ {}_0^{\mathbf{C}}D_t^{(n-1)\alpha} Res_N(0) = {}_0^{\mathbf{C}}D_t^{(n-1)\alpha} Res_{N_n}(0) = 0, \end{aligned}\right\} \forall n = 1, 2, 3, \ldots, . \quad (12)$$

Step 4: Now, the values of a_j, b_j, c_j, and d_j for $j = 1, 2, 3, \ldots, n$ are obtained using Eq. (12).

Step 5: The higher accuracy can be obtained by evaluating more coefficients in Eq. (9).

6.2 Convergence Analysis

This section discusses the convergence analysis of semi-analytical solutions obtained using the RPS method. Let us consider two FPS about $z = z_0$

$$r(z) = \sum_{j=0}^{\infty} l_i (z - z_0)^{j\alpha}, \; r_n(z) = \sum_{j=0}^{n} l_j (z - z_0)^{j\alpha}, \; z_0 \leq z < (z_0 + \rho). \quad (13)$$

Theorem 6.1 *[27] If for* $0 < P < 1$, $|r_{n+1}(z)| \leq P|r_n(z)|$, $\forall n \in \mathbb{N}$ *and* $0 < z < \rho < 1$, *then the solution of an FPS converges to an exact solution.*
Proof: *We have*

$$\begin{aligned} |r(z) - r_n(z)| &= \left| \sum_{j=n+1}^{\infty} r_j(z) \right| \\ &\leq \sum_{j=n+1}^{\infty} |r_j(z)|, \quad \forall\ 0 < z < \rho < 1. \\ &\leq |j_0| \left| \sum_{j=n+1}^{\infty} P^j \right| \\ &= \frac{P^{n+1}}{(1-P)} |j_0| \to 0 \text{ as } n \to \infty. \end{aligned}$$

Theorem 6.2 *[27] The FPS* $\sum_{j=0}^{\infty} l_j z^{j\alpha}$, $z \geq 0$ *has a radius of convergence* $\rho^{\frac{1}{\alpha}}$, *if the classical power series expansion* $\sum_{j=0}^{\infty} l_j z^i$, $-\infty < z < \infty$ *has a radius of convergence* ρ.

6.3 Solution

The parameters and initial conditions of the model (Eq. (3)) are taken as $r_1 = 0.002$, $r_2 = 0.02$, $\lambda = 0.007$, $\mu_1 = 0.009$, $\mu_2 = 0.001$, $\mu_3 = 0.003$, $N_0 = 100$, $S_0 = 75$, $I_0 = 10$, and $R_0 = 15$.

For $n = 1$, from Eq. (7), we get

$$S_1(t) = a_0 + \frac{a_1 t^\alpha}{\Gamma(\alpha+1)}, \quad I_1(t) = b_0 + \frac{b_1 t^\alpha}{\Gamma(\alpha+1)},$$
$$R_1(t) = c_0 + \frac{c_1 t^\alpha}{\Gamma(\alpha+1)}, \quad N_1(t) = d_0 + \frac{d_1 t^\alpha}{\Gamma(\alpha+1)}.$$

Using Step (3), 1^{st}-residual functions of $S(t)$, $I(t)$, $R(t)$, and $N(t)$ are obtained as

$$Res_{S_1}(t) = {}_0^{\mathbf{C}}D_t^\alpha S_1(t) - 0.007N_1(t) + 0.002S_1(t)I_1(t) + 0.009S_1(t),$$
$$Res_{I_1}(t) = {}_0^{\mathbf{C}}D_t^\alpha I_1(t) - 0.002S_1(t)I_1(t) + 0.021I_1(t),$$
$$Res_{R_1}(t) = {}_0^{\mathbf{C}}D_t^\alpha R_1(t) - 0.02I_1(t) + 0.003R_1(t),$$
$$Res_{N_1}(t) = {}_0^{\mathbf{C}}D_t^\alpha N_1(t) - 0.007N_1(t) + 0.009S_1(t) + 0.001I_1(t) + 0.003R_1(t).$$

On substituting $S_1(t)$, $I_1(t)$, $R_1(t)$ and $N_1(t)$ into the previous expression and equating $Res_{S_1}(0)$, $Res_{I_1}(0)$, $Res_{R_1}(0)$, and $Res_{N_1}(0)$ to zero, the values of a_1, b_1, c_1, and d_1 are obtained as

$$a_1 = -0.1250, \ b_1 = -0.0600, \ c_1 = 0.1948, \ \text{and} \ d_1 = 0.0098.$$

Hence, $S_1(t)$, $I_1(t)$, $R_1(t)$, and $N_1(t)$ can be written as

$$S_1(t) = 75 - \frac{0.1250t^\alpha}{\Gamma(\alpha+1)}, \ I_1(t) = 10 - \frac{0.0600t^\alpha}{\Gamma(\alpha+1)},$$
$$R_1(t) = 15 + \frac{0.1948t^\alpha}{\Gamma(\alpha+1)}, \ N_1(t) = 100 + \frac{0.0098t^\alpha}{\Gamma(\alpha+1)}.$$

For $n = 2$, from Eq. (7), we get

$$S_2(t) = 75 - \frac{0.1250t^\alpha}{\Gamma(\alpha+1)} + \frac{a_2 t^{2\alpha}}{\Gamma(2\alpha+1)}, \quad I_2(t) = 10 - \frac{0.0600t^\alpha}{\Gamma(\alpha+1)} + \frac{b_2 t^{2\alpha}}{\Gamma(2\alpha+1)},$$
$$R_2(t) = 15 + \frac{0.1948t^\alpha}{\Gamma(\alpha+1)} + \frac{c_2 t^{2\alpha}}{\Gamma(2\alpha+1)}, \quad N_2(t) = 100 + \frac{0.0098t^\alpha}{\Gamma(\alpha+1)} + \frac{d_2 t^{2\alpha}}{\Gamma(2\alpha+1)}.$$

Now, from Eqs. (11) and (12), we obtain

$$a_2 = 0.0023, \ b_2 = 0.0001, \ c_2 = -0.0013, \ \text{and} \ d_2 = 0.0012.$$

Thus, $S_2(t)$, $I_2(t)$, $R_2(t)$, and $N_2(t)$ can be written as

$$S_2(t) = 75 - \frac{0.1250t^\alpha}{\Gamma(\alpha+1)} + \frac{0.0023t^{2\alpha}}{\Gamma(2\alpha+1)}, \quad I_2(t) = 10 - \frac{0.0600t^\alpha}{\Gamma(\alpha+1)} + \frac{0.0001t^{2\alpha}}{\Gamma(2\alpha+1)},$$
$$R_2(t) = 15 + \frac{0.1948t^\alpha}{\Gamma(\alpha+1)} - \frac{0.0013t^{2\alpha}}{\Gamma(2\alpha+1)}, \quad N_2(t) = 100 + \frac{0.0098t^\alpha}{\Gamma(\alpha+1)} + \frac{0.0012t^{2\alpha}}{\Gamma(2\alpha+1)}.$$

The rest coefficients of Eq. (9) can be obtained using the following recurrence relations

$$\left.\begin{aligned} a_{j+1} &= \lambda d_j - r_1\sum_{r=0}^{j}\frac{a_r b_{j-r}\Gamma(j\alpha+1)}{\Gamma(r\alpha+1)\Gamma((j-r)\alpha+1)} - \mu_1 a_j,\\ b_{j+1} &= r_1\sum_{r=0}^{j}\frac{a_r b_{j-r}\Gamma(j\alpha+1)}{\Gamma(r\alpha+1)\Gamma((j-r)\alpha+1)} - (r_2+\mu_2)b_j,\\ c_{j+1} &= r_2 b_j - \mu_3 c_j,\ d_{j+1} = \lambda d_j - \mu_1 a_j - \mu_2 b_j - \mu_3 c_j, \end{aligned}\right\}\forall j = 1, 2\ldots, n. \tag{14}$$

7 Results and Discussion

To show the convergence of the method (From Eqs. (6), (7) and (13)), values of $|S(t) - S_n(t)|$, $|I(t) - I_n(t)|$, $|R(t) - R_n(t)|$, and $|N(t) - N_n(t)|$ at $t = 0.99$ with respect to n are plotted in Figs. 2a to 2d for different values of $\alpha = 1.0, 0.99, 0.95, 0.9$, and 0.85. It is observed that maximum absolute error $\mathcal{O}(10^{-45})$ is obtained for $n = 20$. For $n = 10$, the maximum absolute errors is $\mathcal{O}(10^{-20})$. In subsequent calculations, we use $n = 10$, as it gives sufficient accuracy.

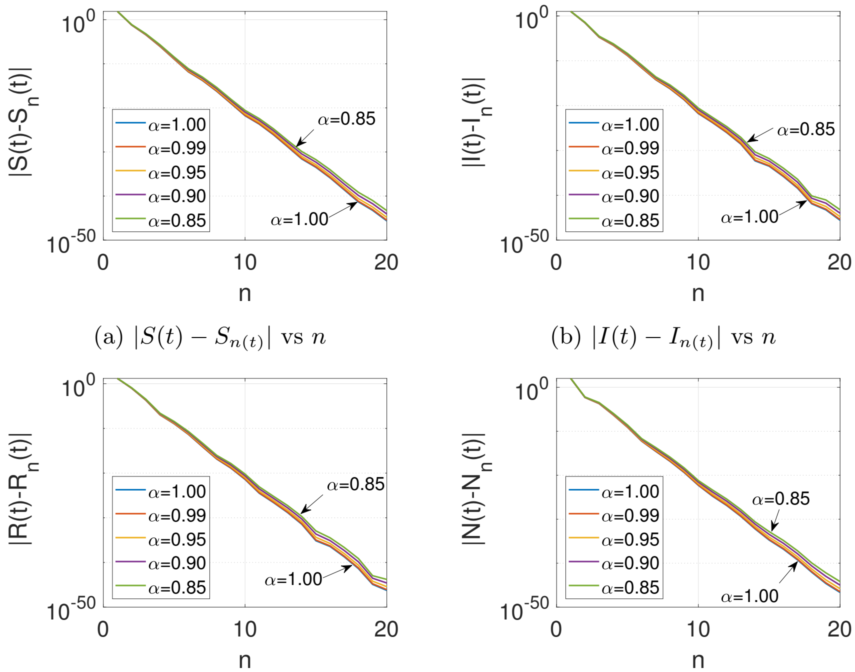

(a) $|S(t) - S_{n(t)}|$ vs n

(b) $|I(t) - I_{n(t)}|$ vs n

(c) $|R(t) - R_{n(t)}|$ vs n

(d) $|N(t) - N_{n(t)}|$ vs n

Figure 2: Convergence analysis of the RPS approach at $t = 0.99$ for distinct fractional orders $\alpha \in (0, 1]$.

For $\alpha = 1$ and $n = 10$, the absolute errors between RK and RPS methods in $S(t)$, $I(t)$, $R(t)$, and $N(t)$ are denoted by $Abs_S(t)$, $Abs_I(t)$, $Abs_R(t)$, and $Abs_N(t)$, respectively, which are defined as

$$\left.\begin{array}{ll} Abs_S(t) = |S(t)_{RK} - S(t)_{RPS}|, & Abs_I(t) = |I(t)_{RK} - I(t)_{RPS}|, \\ Abs_R(t) = |R(t)_{RK} - R(t)_{RPS}|, & Abs_N(t) = |N(t)_{RK} - N(t)_{RPS}|, \end{array}\right\} t \geq 0. \tag{15}$$

For fractional order $\alpha = 1$ and $n = 10$, comparison between the RK and RPS solutions in $S(t)$, $I(t)$, $R(t)$, and $N(t)$ are shown in Table I. Further, the absolute errors in $S(t)$, $I(t)$, $R(t)$, and $N(t)$ using the RPS and RK methods for $\alpha = 1$ are depicted in Figs. 3a to 3d. Here, maximum absolute errors in $S(t)$, $I(t)$, $R(t)$, and $N(t)$ are $\mathcal{O}(10^{-13})$ for $t \in (0, 1]$.

Table I and Figs. 3a to 3d show that the RPS method gives accurate and reliable results for a minimal computational coefficients.

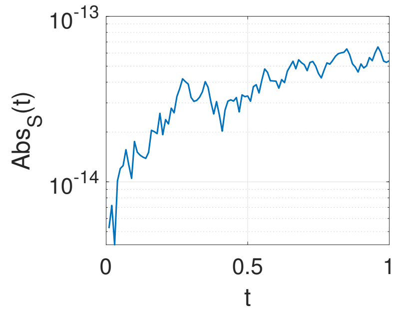

(a) $Abs_S(t)$ vs t

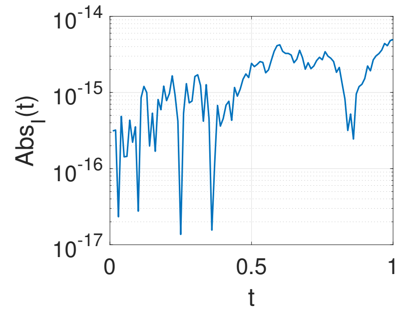

(b) $Abs_I(t)$ vs t

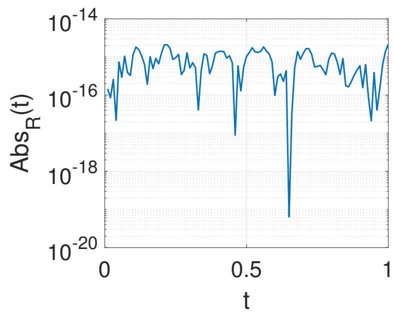

(c) $Abs_I(t)$ vs t

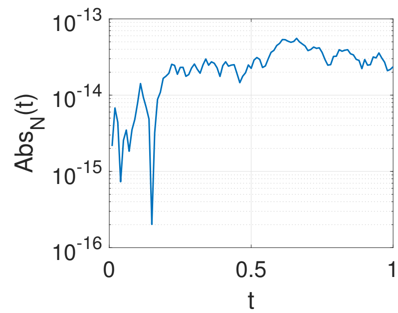

(d) $Abs_N(t)$ vs t

Figure 3: Absolute error of $S(t)$, $I(t)$, $R(t)$, and $N(t)$ using RK and RPS methods, respectively, for $\alpha = 1$ and $n = 10$.

Table I: The values of $S(t)$, $I(t)$, $R(t)$, and $N(t)$ using RK and RPS methods for $\alpha = 1$ (upto 3 decimal places).

	RK method				RPS method			
t	$S(t)$	$I(t)$	$R(t)$	$N(t)$	$S(t)$	$I(t)$	$R(t)$	$N(t)$
0	75.0	10.0	15.0	100.0	75.0	10.0	15.0	100.0
0.1	74.988	9.994	15.019	100.001	74.988	9.994	15.019	100.001
0.2	74.975	9.988	15.039	100.002	74.975	9.988	15.039	100.002
0.3	74.963	9.982	15.058	100.003	74.963	9.982	15.058	100.003
0.4	74.950	9.976	15.078	100.004	74.950	9.976	15.078	100.004
0.5	74.938	9.970	15.097	100.005	74.938	9.970	15.097	100.005
0.6	74.925	9.964	15.117	100.006	74.925	9.964	15.117	100.006
0.7	74.913	9.958	15.136	100.007	74.913	9.958	15.136	100.007
0.8	74.901	9.952	15.155	100.008	74.901	9.952	15.155	100.008
0.9	74.888	9.946	15.175	100.009	74.888	9.946	15.175	100.009
1.0	74.876	9.940	15.194	100.010	74.876	9.940	15.194	100.010

Table II: The values of $S(t)$, $I(t)$, $R(t)$, and $N(t)$ via RPS method (upto 3 decimal places).

	RPS ($\alpha = 0.80$)				RPS ($\alpha = 0.70$)			
t	$S(t)$	$I(t)$	$R(t)$	$N(t)$	$S(t)$	$I(t)$	$R(t)$	$N(t)$
0	75.0	10.0	15.0	100.0	75.0	10.0	15.0	100.0
0.1	74.979	9.990	15.033	100.001	74.973	9.987	15.043	100.002
0.2	74.963	9.982	15.058	100.003	74.956	9.979	15.069	100.004
0.3	74.949	9.975	15.080	100.004	74.941	9.972	15.092	100.005
0.4	74.936	9.969	15.100	100.005	74.928	9.965	15.112	100.006
0.5	74.923	9.963	15.120	100.006	74.916	9.959	15.132	100.007
0.6	74.912	9.957	15.138	100.007	74.905	9.954	15.149	100.008
0.7	74.900	9.952	15.157	100.008	74.894	9.949	15.166	100.009
0.8	74.889	9.946	15.174	100.009	74.884	9.944	15.182	100.010
0.9	74.878	9.941	15.191	100.010	74.874	9.939	15.198	100.011
1.0	74.867	9.936	15.208	100.011	74.864	9.934	15.213	100.012

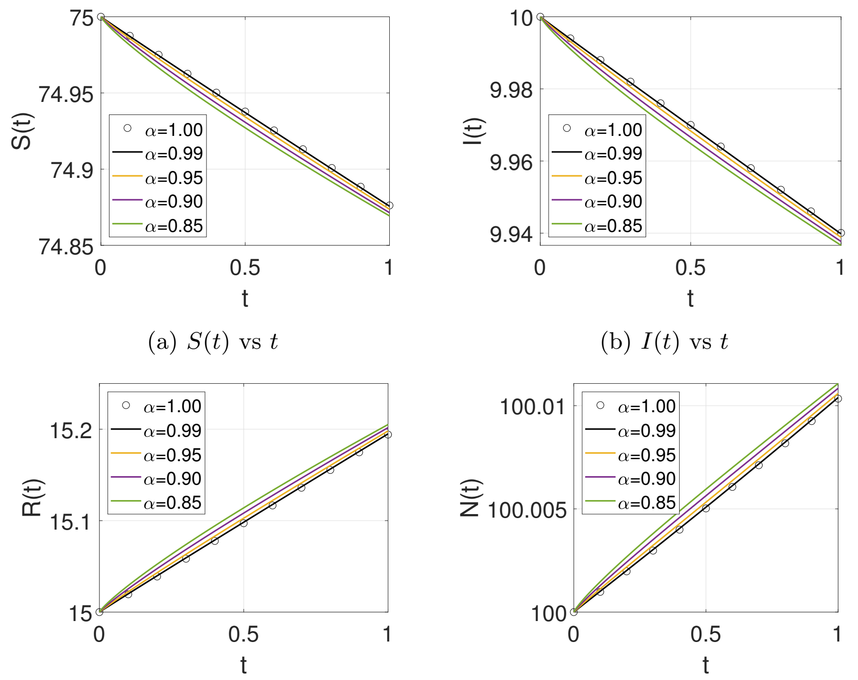

(a) $S(t)$ vs t (b) $I(t)$ vs t (c) $R(t)$ vs t (d) $N(t)$ vs t

Figure 4: The semi-analytical solutions of $S(t)$, $I(t)$, $R(t)$, $N(t)$ for distinct fractional orders $\alpha \in (0, 1]$ and $n = 10$.

The RPS solution of $S(t)$, $I(t)$, $R(t)$, and $N(t)$ for $\alpha = 0.80$ and 0.70 are listed in Table II. The behavior of $S(t)$, $I(t)$, $R(t)$, and $N(t)$ for distinct fractional order $\alpha \in (0, 1]$ is depicted in Figs. 4a to 4d, respectively. These figures show that the number of susceptible and infected individuals decreases with a decrease in α. At the same time, an increase in the recovered and total population is observed with a decrease in α.

8 Conclusion

In this paper, we have developed the SIR model (Eq. (3)) with vital dynamics and variable population sizes for integer and fractional orders. Further, we have discussed the existence and uniqueness of the solutions for the stable model. After that, the semi-analytical solutions for the proposed model are obtained by the RPS approach. For $\alpha = 1$, we have compared the results obtained by RPS and the RK methods. The convergence analysis of the RPS technique is also discussed. It is also observed that with the decline in fractional order (α), the numbers of susceptible and infected decrease, while the numbers of recovered personnel and the total population increase. Numerical simulation and graphs show that the fractional SIR epidemic model with vital dynamics and variable population size gives a better understanding and produces outstanding results than an integer SIR epidemic model without vital dynamics and varying population size. The results indicate that the RPS technique can be used as an alternative method for solving linear and nonlinear differential equations of any arbitrary order. This study may be helpful for medical experts in controlling the infection during the disease.

Acknowledgements

The Junior Research Fellowship (JRF) provided by the Council of Scientific & Industrial Research (CSIR), New Delhi, India, via file no: $09/1007(0011)/2021-EMR-I$ during the study of present work is acknowledged by the first author.

References

[1] S. Dubey, V. P. Dubey, J. Singh, A. M. Alshehri, D. Kumar, Computational study of a local fractional Tricomi equation occurring in fractal transonic flow, *J. Comput. Nonlinear Dyn.* 17 (8) (2022) 081006.

[2] V. P. Dubey, D. Kumar, H. M. Alshehri, J. Singh, D. Baleanu, Generalized invexity and duality in multiobjective variational problems involving non-singular fractional derivative, *Open Phys.* 20 (1) (2022) 939–962.

[3] Akshey, T. R. Singh, A robust iterative approach for space-time fractional multidimensional telegraph equation, *Int. J. Appl. Comput.* 9 (5) (2023) 84.

[4] I. Podlubny, A. Chechkin, T. Skovranek, Y. Chen, B. M. V. Jara, Matrix approach to discrete fractional calculus II: partial fractional differential equations, *J. Comput. Phys.* 228 (8) (2009) 3137–3153.

[5] V. P. Dubey, J. Singh, S. Dubey, D. Kumar, Some integral transform results for Hilfer–Prabhakar fractional derivative and analysis of free-electron laser equation, *Iranian J. Sci.* 47 (4) (2023) 1333–1342.

[6] V. P. Dubey, J. Singh, S. Dubey, D. Kumar, Analysis of cauchy problems and diffusion equations associated with the Hilfer–Prabhakar fractional derivative via Kharrat–Toma transform, *Fractal fract.* 7 (5) (2023) 413.

[7] D. Kumar, V. P. Dubey, S. Dubey, J. Singh, A. M. Alshehri, Computational analysis of local fractional partial differential equations in realm of fractal calculus, *Chaos Solit. Fractals* 167 (2023) 113009.

[8] V. P. Dubey, D. Kumar, S. Dubey, A modified computational scheme and convergence analysis for fractional order hepatitis E virus model, in: *Advanced Numerical Methods for Differential Equations*, CRC Press, 2021, pp. 279–312.

[9] V. P. Dubey, J. Singh, A. M. Alshehri, S. Dubey, D. Kumar, Forecasting the behavior of fractional order Bloch equations appearing in NMR flow via a hybrid computational technique, *Chaos Solit. Fractals* 164 (2022) 112691.

[10] V. P. Dubey, J. Singh, A. M. Alshehri, S. Dubey, D. Kumar, Numerical investigation of fractional model of phytoplankton–toxic phytoplankton–zooplankton system with convergence analysis, *Int. J. Biomath.* 15 (04) (2022) 2250006.

[11] H. W. Hethcote, P. van den Driessche, An SIS epidemic model with variable population size and a delay, *J. Math. Biol.* 34 (1995) 177–194.

[12] A. S. Ackleh, L. J. Allen, Competitive exclusion and coexistence for pathogens in an epidemic model with variable population size, *J. Math. Biol.* 47 (2003) 153–168.

[13] G. Zaman, Y. H. Kang, I. H. Jung, Stability analysis and optimal vaccination of an SIR epidemic model, *BioSystems* 93 (3) (2008) 240–249.

[14] H. El-Saka, The fractional-order SIR and SIRS epidemic models with variable population size, *Math. Sci. Lett.* 2 (3) (2013) 195.

[15] E. A. Bakare, A. Nwagwo, E. Danso-Addo, Optimal control analysis of an SIR epidemic model with constant recruitment, *Int. J. Appl. Math. Research* 3 (3) (2014) 273.

[16] M. Hassouna, A. Ouhadan, E. El Kinani, On the solution of fractional order SIS epidemic model, *Chaos Solit. Fractals* 117 (2018) 168–174.

[17] A. Taghvaei, T. T. Georgiou, L. Norton, A. Tannenbaum, Fractional SIR epidemiological models, *Sci. Reports* 10 (1) (2020) 20882.

[18] K. Kozioł, R. Stanisławski, G. Bialic, Fractional-order SIR epidemic model for transmission prediction of covid-19 disease, *Appl. Sci.* 10 (23) (2020) 8316.

[19] Y. Chen, F. Liu, Q. Yu, T. Li, Review of fractional epidemic models, *Appl. Math. Model.* 97 (2021) 281–307.

[20] C. Balzotti, M. D'Ovidio, A. C. Lai, P. Loreti, Effects of fractional derivatives with different orders in SIS epidemic models, *Computation* 9 (8) (2021) 89.

[21] R. K. Meena, S. Kumar, Solution of fractional order SIR epidemic model using residual power series method, *Palest. J. Math.* 11 (2022).

[22] R. K. Meena, S. Kumar, A study on fractional SIS epidemic model using RPS method, in: *International Conference on Mathematics and Computing*, Springer, 2023, pp. 293–309.

[23] M. R. Sidi Ammi, M. Tahiri, M. Tilioua, A. Zeb, I. Khan, M. Andualem, Global analysis of a time fractional order spatio-temporal SIR model, *Sci. Rep.* 12 (1) (2022) 5751.

[24] M. Sadki, S. Harroudi, K. Allali, Fractional-order SIR epidemic model with treatment cure rate, *Partial Differ. Equ. Appl. Math.* 8 (2023) 100593.

[25] I. Podlubny, Fractional differential equations: an introduction to fractional derivatives, fractional differential equations, to methods of their solution and some of their applications, Elsevier, (1998).

[26] A. A. Kilbas, H. M. Srivastava, J. J. Trujillo, Theory and applications of fractional differential equations, Vol. 204, Elsevier, 2006.

[27] A. El-Ajou, O. A. Arqub, Z. A. Zhour, S. Momani, New results on fractional power series: theories and applications, *Entropy* 15 (12) (2013) 5305–5323.

[28] A. M. El-Sayed, On the existence and stability of positive solution for a nonlinear fractional-order differential equation and some applications, *Alex. J. Math.* 1 (1) (2010) 1–10.

[29] A. El-Ajou, O. A. Arqub, M. Al-Smadi, A general form of the generalized Taylor's formula with some applications, *Appl. Math. Comput.* 256 (2015) 851–859.

[30] K. Moaddy, M. Al-Smadi, I. Hashim, A novel representation of the exact solution for differential algebraic equations system using residual power-series method, *Discrete Dyn. Nat. Soc.* 2015 (2015).

[31] L. Wang, X. Chen, Approximate analytical solutions of time fractional Whitham–Broer–Kaup equations by a residual power series method, *Entropy* 17 (9) (2015) 6519–6533.

[32] R. Abu-Gdairi, M. Al-Smadi, G. Gumah, An expansion iterative technique for handling fractional differential equations using fractional power series scheme, *J. Math. Stat.* 11 (2) (2015) 29.

[33] I. Komashynska, M. Al-Smadi, A. Al-Habahbeh, A. Ateiwi, Analytical approximate solutions of systems of multi-pantograph delay differential equations using residual power-series method, arXiv preprint arXiv:1611.05485 (2016).